

Reaction Condition Effects on Nickel Sorption Mechanisms in Illite–Water Suspensions

E. J. Elzinga* and D. L. Sparks

ABSTRACT

Nickel sorption in illite suspensions was studied as a function of pH (4.5–8.0), reaction time (3 h, 24 h, and 1 wk) and ionic strength ($I = 0.1$ and $0.003 M$) using x-ray absorption spectroscopy (XAS) to characterize the Ni sorption complexes formed. The formation of Ni–Al layered double hydroxide (LDH) phases was observed at pH values >6.25 , with increasing formation of these phases with time, and a faster formation rate with increasing pH. Comparison among samples with the same Ni loading, but different reaction times and pH values, showed larger second neighbor scattering for the samples reacted at higher pH, which had a faster Ni sorption rate. Most likely this was due to a greater importance of Ni–Al LDH precipitation relative to other (mononuclear) Ni sorption mechanisms at higher pH, and/or a higher Al content in the Ni–Al LDH phase formed at lower pH (slower Ni sorption rate). Lowering the ionic strength resulted in increased Ni sorption for the entire pH range studied. Our extended x-ray absorption fine structure spectroscopy (EXAFS) data indicated that this was due to significant outer-sphere Ni sorption occurring at the planar sites at low I , leading to a reduced importance of Ni–Al LDH formation in the overall Ni sorption process at pH > 6.50 .

RETENTION of heavy metal ions by soil minerals is a crucial process for maintaining environmental quality in contaminated areas. Sorption reactions at solid–water interfaces decrease solute mobility and often control the fate, bioavailability, and transport of trace metal ions such as Ni in aquatic and soil environments. Correctly determining the mechanisms of metal sorption to clay minerals such as illite is therefore of great importance for understanding the fate of metals in contaminated soils and sediments, and may help in optimizing environmental remediation procedures by accounting for the metal speciation in soils.

Illite is a 2:1 phyllosilicate mineral with tightly held, nonhydrated, interlayer K cations balancing a high layer charge (Fanning et al., 1989). Illitic clays are often an important constituent of the solid phase in alluvial soils and in arid zone soils (Bolt et al., 1979; Fanning et al., 1989). As with many clay minerals, illite contains both planar and edge sites available for metal uptake. Planar sites are due to a net negative structural charge resulting from isomorphic substitution in the octahedral and tetrahedral sheets, and edge sites are due to broken Al–OH and Si–OH bonds at the edges of the clay crystallite (McBride, 1994). The presence of planar sites in illitic clays presumably results in part from interstratified vermiculite and smectite layers (Srodon and Eberl, 1984), which form if the clay is brought in contact with a solution of low K concentration. Upon prolonged exposure

to this solution, the edge-situated interlattice sites become occupied by ions other than K, presumably leading to partial opening of the interlattice space (Bolt et al., 1979).

The different sites available for metal uptake by illite may lead to different Ni retention mechanisms occurring in Ni–illite systems. The planar sites constitute permanent negative charge. Metal interactions with these sites are electrostatic in nature and lead to the formation of outer-sphere metal complexes; that is, the metal ions do not lose their primary hydration spheres upon interaction with the clay mineral surface (Sposito, 1989; Sparks, 1995). At the illite edge sites, both the formation of outer-sphere complexes and chemisorption may occur. Chemisorption leads to the formation of inner-sphere metal complexes through a ligand exchange process, where the metal ions form chemical bonds with the clay mineral surface by coordination to surface hydroxy ligands (Sposito, 1989). Since illite is an Al-containing clay mineral, the formation of Ni–Al LDH phases may also be expected. The importance of the formation of these precipitates has recently been demonstrated in spectroscopic studies of Ni sorption to Al-bearing clay minerals and oxides (d’Espinoise de la Caillerie et al., 1995; Scheidegger et al., 1998; Scheinost et al., 1999). These phases are typically observed in a pH range below the pH where the solubility of β -Ni(OH)₂ precipitates is exceeded. In the case of Ni sorption to pyrophyllite and other Al-bearing minerals described by Scheinost et al. (1999), the Ni phase that formed was unequivocally identified as a mixed Ni–Al LDH sheet, where the Al originated from the sorbent structure.

In the following the term *sorption* is used to describe the surface-mediated removal of Ni cations from solution. This includes adsorption processes at the illite clay sites and planar sites (i.e., formation of mononuclear inner- and outer-sphere Ni sorption complexes), as well as formation of Ni–Al LDH precipitates, which incorporate Al dissolved from the illite structure. Studies employing transmission electron microscopy showed that Co–Al LDH phases do not form coatings on Al₂O₃ and kaolinite surfaces but rather form three-dimensional precipitate clusters that lack a preferred orientation with respect to the surfaces of these minerals, and in some cases are detached from the surface (Towle et al., 1997; Thompson et al., 1999). These results indicate that formation of Co–Al LDH is not a result of surface crowding; that is, the precipitates do not consist of sorbed metal ions nucleated with metal ions on adjacent surface sites, since this would result in precipitate coatings on the mineral surface. For this reason, Ni–Al LDH forma-

Dep. of Plant and Soil Sciences, Univ. of Delaware, Newark, DE 19717-1303; E.J. Elzinga, Dep. of Geosciences, State Univ. of New York, Stony Brook, NY 11794-2100. Received 24 Aug. 1999. *Corresponding author (elzinga@udel.edu).

Abbreviations: BET, Brunauer–Emmett–Teller; EGME, ethylene glycol mono-ethyl ether; EXAFS, extended x-ray absorption fine structure spectroscopy; LDH, layered double hydroxide; RSF, radial structure functions.

tion may be considered as a separate sorption mechanism that occurs simultaneously with, and therefore competes with, adsorption processes at the illite planar and edge sites (i.e., formation of inner- and outer-sphere Ni sorption complexes), instead of Ni-Al LDH precipitates being the products formed at these sites at high Ni loadings. The Ni sorption densities of the samples will be reported based on the total surface area of the illite clay. This was done only to allow for convenient comparison of the Ni sorption levels in the Ni-illite samples and not to imply a certain distribution of the Ni atoms at the illite surface.

In this study, we present macroscopic and spectroscopic data on Ni sorption in illite suspensions. As discussed above, Ni sorption in illite suspensions may proceed via a number of different mechanisms. The Ni speciation in illite suspensions will therefore be determined by how effective each of the different sorption mechanisms competes for Ni uptake, which may be affected by a range of experimental parameters, including pH, reaction time, and ionic strength. Therefore, rather than limiting our systems to a single set of experimental parameters, we studied Ni sorption to illite as a function of pH, reaction time, and ionic strength to determine the effect of these experimental parameters on the Ni sorption products formed in illite suspensions. X-ray absorption spectroscopy was used to characterize the sorbed Ni bonding environment at the molecular scale.

MATERIALS AND METHODS

The experiments were performed with Silver Hill Illite, Imt-1, obtained from the Source Clay Minerals Repository at the University of Missouri, Columbia, MO. After grinding in a ball mill for 2 wk, the material was treated for removal of Ca carbonates, Fe oxides, and organic matter following the procedures described in Jackson (1956). We used the $<2 \mu\text{m}$ fraction, which was isolated by sedimentation, and then saturated with Na. The clay was dialyzed for removal of excess salts and freeze-dried. The surface area of the clay was determined by both the N_2 -Brunauer-Emmett-Teller (BET) method and the ethylene glycol mono-ethyl ether (EGME) method. The N_2 -BET surface area was $17 \text{ m}^2 \text{ g}^{-1}$, and the EGME surface area was $163 \text{ m}^2 \text{ g}^{-1}$. The difference between both methods indicates that a substantial amount of smectite-like phases was present in our illite clay fraction, consistent with the description of this illite by Srodon and Eberl (1984) as a mixture of illite and illite-smectite phases.

The sorption of Ni to illite was studied in batch experiments, using polyethylene reaction vessels. The following experimental parameters were varied: (i) pH: 4.5 to 8.0; (ii) pH control: constant and drifting pH over time; (iii) ionic strength: 0.1 and 0.003 M NaNO_3 ; and (iv) reaction time: 3 h, 24 h, and 1 wk. All studies were conducted under an N_2 atmosphere to eliminate effects of CO_2 . The solid/solution ratio was 2 g L^{-1} , and the initial Ni concentration was 1 mM.

Metal sorption in mineral suspensions is often studied in systems where pH is not kept at a constant value during the time allowed for equilibration (e.g., Benjamin and Leckie, 1982; Roe et al., 1991; Zachara et al., 1993; O'Day et al., 1996). In these systems, pH drifts due to metal sorption and sorbent mineral dissolution until equilibrium is reached. In the case of Ni sorption to clay minerals, both the Ni sorption reaction (Scheidegger et al., 1998; Roberts et al., 1999; Scheinost et al., 1999) and the sorbent dissolution reaction (Scheidegger et al.,

1997; Ford et al., 1999) may take weeks to reach equilibrium, during which time pH continuously drifts. Since pH is an important variable that may control both the extent and the mechanism of metal sorption (Bargar et al., 1998; Strawn and Sparks, 1999; Roberts et al., 1999), pH drift may affect the metal sorption product formed. We have studied the effect of pH drift on the Ni sorption mechanisms on illite by comparing the macroscopic and spectroscopic data obtained from systems where pH was not controlled to those from systems where pH was held at a constant value over time. In the system with pH drift, different amounts of acid (0.1 M HNO_3) or base (0.1 M NaOH) were added to the Ni-illite suspensions at the beginning of the experiment, and pH and the Ni concentration remaining in solution were measured after 1 and 8 d of reaction.

In the pH controlled system, pH was held constant by either using a pH stat apparatus (samples with $\text{pH} > 5$ in the $I = 0.003 \text{ M}$ system), manual addition of 0.1 M HNO_3 or 0.1 M NaOH twice a day ($\text{pH} = 4.5$ and 5.0 in both $I = 0.1$ and 0.003 M systems), or by using a 0.05 M MES ($\text{pH} = 5.5$ – 6.5) or 0.05 M HEPES ($\text{pH} = 6.75$ – 8.0) buffer concentration in the background electrolyte ($I = 0.1 \text{ M}$ system). MES and HEPES are organic buffers with pK_a values of 6.1 and 7.5, respectively. Preliminary studies showed no differences in Ni sorption as a function of time between Ni-illite systems equilibrated on a pH stat at $\text{pH} = 5.5$ and 7.5 and Ni-illite systems where pH was maintained constant by using 0.05 M MES ($\text{pH} = 5.5$) or 0.05 M HEPES ($\text{pH} = 7.5$) in the background electrolyte. This indicated that the organic buffers did not interfere with the Ni sorption process(es) in the illite suspensions, which is consistent with results of other metal sorption studies using MES and organic buffers similar to HEPES (Baeyens and Bradbury, 1995; Strawn et al., 1998).

The buffer solutions were prepared by titrating a 0.05 M buffer solution to the desired pH using a 10 M NaOH solution, and then adding an appropriate amount of $\text{NaNO}_3(\text{s})$ to achieve a final $I = 0.1 \text{ M}$. The needed amount of $\text{NaNO}_3(\text{s})$ was calculated by accounting for the buffer speciation at the pH value of interest, and the Na concentration resulting from the amount of 10 M NaOH added to reach this pH.

The $I = 0.1 \text{ M}$ NaNO_3 suspensions were hydrated for 24 h by stirring while open to a N_2 glove box atmosphere. Next, an appropriate amount of 0.1 M $\text{Ni}(\text{NO}_3)_2$ was added to achieve an initial Ni concentration of 1 mM. For the system with noncontrolled pH, 0.1 M HNO_3 , or 0.1 M NaOH was added (prior to Ni addition) in different amounts to each sample. The suspensions were then sealed, placed in gas tight zipper bags inside the glove box, and transferred to a reciprocal shaker outside the glove box for equilibration. The $I = 0.003 \text{ M}$ NaNO_3 suspensions were hydrated on a reciprocal shaker for 22 h and then placed on the pH-stat apparatus. The suspensions were vigorously stirred with a magnetic stir bar and purged with N_2 to eliminate CO_2 . The pH was maintained at the desired value using 0.1 M NaOH. After 2 h, an appropriate amount of Ni from a 0.1 M $\text{Ni}(\text{NO}_3)_2$ stock solution was added to achieve an initial Ni concentration of 1 mM.

Subsamples from the $I = 0.1$ and 0.003 M systems were taken at the reaction times of interest. The samples were centrifuged and the supernatants were passed through a $0.2\text{-}\mu\text{m}$ filter. The filtered supernatants were then acidified and analyzed by inductively coupled plasma spectrometry for Ni. Nickel sorption was determined from the difference between the initial and final Ni concentrations.

The solids from select samples were analyzed by EXAFS spectroscopy. The wet pastes were not washed to remove entrained electrolyte since in all samples the amount of Ni sorbed at the mineral surface was at least ≈ 50 times higher

than the amount of Ni in the entrained electrolyte. The samples were sealed and stored in a refrigerator to keep them moist for EXAFS analysis.

The EXAFS spectra were recorded at Beamline X-11A of the National Synchrotron Light Source, Brookhaven National Laboratory, Upton, NY. The electron storage ring was operated at 2.5 GeV with an average beam current of 180 mA. A Si(111) crystal was used as the monochromator. The premonochromator slit width was 0.5 mm, which yielded a resolution of ≈ 0.5 eV. Higher order harmonics were suppressed by detuning 25% from the maximum beam intensity at 900 eV above the Ni K-edge of 8333 eV.

The samples were scanned in fluorescence mode at the Ni K-edge using a Lytle detector. The samples were placed at a 45° angle to the incident beam, and a wide-angle collector with an ionization chamber was located at 90° off the incident beam. Fill-gases used were Ar for the Lytle detector and N₂ for the I₀ detector. A Co filter and soller slits were placed between the sample and the detector to reduce elastically scattered x-rays entering the fluorescence detector. The spectra were collected at room temperature. Three scans were collected per sample to improve the signal/noise ratio.

Background subtraction, Fourier filtering, and data fitting were accomplished with the program MacXAFS 4.0 (Bouldin et al., 1995). The χ function was extracted from the raw data by fitting a linear function to the pre-edge region and a spline function to the post-edge region, and normalizing the edge jump to unity. The data were then converted from energy to k space and weighted by k^3 to compensate for the dampening of the EXAFS amplitude with increasing k .

Data fitting was done in R space. Ab initio amplitude and phase functions for single shells were calculated using the FEFF7 code (Zabinsky et al., 1995), in combination with ATOMS. Reference compounds used were β -Ni(OH)₂ (Johnson Matthey Co.), and α -Ni(OH)₂ prepared as described by Génin et al. (1991). The amplitude reduction factor was 0.83, as determined from fits to the experimental data of the reference compounds. Multishell fitting was done over $\Delta R = 1.07$ to 3.12 Å with $\Delta k = 3.2$ to 13.6 Å⁻¹. For samples having only one shell, single shell fitting was performed over $\Delta R = 1.07$ to 2.30 Å with $\Delta k = 3.2$ to 13.6 Å⁻¹. The Debye-Waller factors of the Ni-Ni and Ni-Al shells were fixed at 0.005 Å² in the case of multishell fitting. This constraint was proposed by Scheidegger et al. (1998) for fitting Ni-Al LDH precipitates. The resulting optimized $R_{\text{Ni-O}}$ and $R_{\text{Ni-Ni}}$ values are estimated to be accurate to ± 0.02 Å, and the $N_{\text{Ni-O}}$ and $N_{\text{Ni-Ni}}$ values are estimated to be accurate to $\pm 20\%$. The estimated accuracies for $N_{\text{Ni-Al}}$ and $R_{\text{Ni-Al}}$ are $\pm 60\%$ and ± 0.06 Å, respectively. A discussion on the fitting procedure employed here and the accuracy estimates is given in Scheidegger et al. (1998). The deviation between the fitted and experimental spectra was quantified as

$$\text{Res}_i = \frac{\sum_{i=1}^N |y_{\text{exp}}(i) - y_{\text{fit}}(i)|}{\sum_{i=1}^N y_{\text{exp}}(i)}$$

where N represents the number of data points, and y_{exp} and y_{fit} are the experimental and theoretical data points, respectively.

RESULTS AND DISCUSSION

EXAFS Data

Figure 1 shows the normalized, background-subtracted and k^3 -weighted EXAFS spectra that were collected for this study. The sorption density, Γ , is indicated

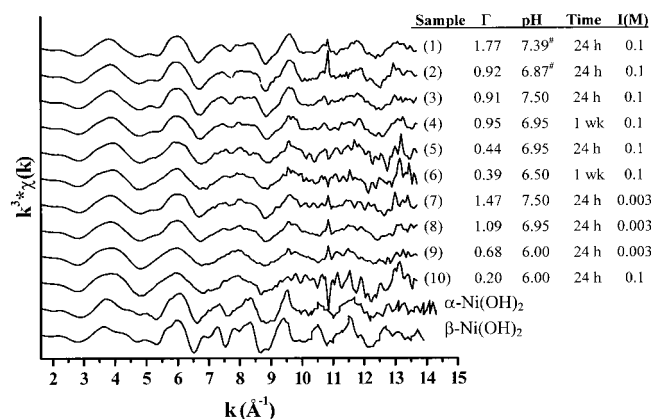


Fig. 1. The k^3 -weighted χ spectra of the samples analyzed extended x-ray absorption fine structure spectroscopy (EXAFS) in this study. The gray circle in Sample 2 locates the cut-off beat characteristic of Ni-Al LDH. Γ is the Ni sorption density (in $\mu\text{mol m}^{-2}$) calculated based on the ethylene glycol mono-ethyl ether (EGME) surface area; # indicates samples with drifting pH over time.

along with the reaction conditions (pH, I , and reaction time) for each sample. The low pH Samples 9 and 10 are dominated by the sinusoid resulting from O backscattering from the first coordination shell of sorbed Ni. In the other samples, additional frequencies appear in the spectra due to the presence of Ni in the second coordination shell of the central Ni atom, which indicates that a Ni precipitate phase is present in these samples (Scheidegger et al., 1998; d'Espinoze et al., 1995). The cut-off beat at ≈ 8 Å⁻¹ recognizable for Samples 1 to 4, and absent in the spectra of β -Ni(OH)₂ and α -Ni(OH)₂, identifies the Ni precipitates formed in the Ni-illite systems as Ni-Al LDH phases (Scheinost and Sparks, 2000). The differences between the EXAFS spectra presented in Fig. 1 indicate that the Ni bonding environment varies as a function of reaction conditions. Since EXAFS provides the average bonding environment of all sorbed Ni atoms, this may be due to variable relative amounts of Ni bound in Ni-Al LDH vs. mononuclear adsorbed Ni species. Additionally, there may be differences between samples with respect to the composition or size of the Ni-Al LDH crystallites.

The structural parameters obtained from EXAFS data fitting are presented in Table 1. The fit results for the Ni-O shell are essentially the same for all samples, with a radial distance of ≈ 2.05 Å, and a coordination number of about six. This indicates that Ni is present in an octahedral environment surrounded by six O atoms in all samples. The radial distance of the Ni-Ni shell is ≈ 3.05 Å in all samples and is typical of Ni-Al LDH (Scheinost and Sparks, 2000). Differences exist in the Ni-Ni coordination numbers, indicating that the reaction conditions affected the amount and/or composition of the Ni-Al LDH phases formed. The radial distance of the Ni-Al shell is ≈ 3.10 Å in all samples, consistent with the results of Scheidegger et al. (1998).

In the following material, the effects of pH, pH control, reaction time and ionic strength on the Ni sorption products formed in the illite suspensions will be discussed using the radial structure functions (RSFs) obtained by Fourier transformation of the k^3 -weighted

Table 1. Structural parameters derived from x-ray absorption spectroscopy analysis.

Sample§	pH	Time	$I(M)$	Γ	Ni-O Shell†			Ni-Ni Shell†			Ni-Al Shell‡			Res	
					$R\ \$	$N\#$	$\sigma^{2\dagger\dagger}$	R	N	σ^2	R	N	σ^2		
				$\mu\text{mol m}^{-2}$	\AA		\AA		\AA^2	\AA		\AA^2			
1	7.39	24 h	0.1	1.77	2.04	5.7	0.004	3.06	4.1	0.005	3.09	0.6	0.005	0.021	
2	6.87	24 h	0.1	0.92	2.05	6.2	0.004	3.05	4.0	0.005	3.09	1.2	0.005	0.084	
3	7.50	24 h	0.1	0.95	2.04	6.0	0.004	3.06	3.7	0.005	3.10	0.7	0.005	0.045	
4	6.95	1 wk	0.1	0.90	2.04	6.0	0.005	3.06	3.2	0.005	3.10	1.5	0.005	0.036	
5	6.95	24 h	0.1	0.44	2.06	5.7	0.003	3.04	2.5	0.005	3.11	1.3	0.005	0.074	
6	6.50	1 wk	0.1	0.39	2.06	5.6	0.004	3.06	1.8	0.005	3.11	1.6	0.005	0.058	
7	7.50	24 h	0.003	1.47	2.04	6.1	0.005	3.06	2.7	0.005	3.10	1.2	0.005	0.035	
8	6.95	24 h	0.003	1.09	2.04	5.9	0.004	3.05	2.3	0.005	3.09	1.5	0.005	0.021	
9	6.00	24 h	0.003	0.68	2.05	6.0	0.004	—	—	—	—	—	—	0.034	
10	6.00	24 h	0.1	0.20	2.05	5.6	0.003	—	—	—	—	—	—	0.18	
					$\alpha\text{-Ni(OH)}_2$	2.04	5.6	0.003	3.09	5.7	0.005	—	—	—	0.068
					$\beta\text{-Ni(ON)}_2$	2.06	5.6	0.002	3.12	7.4	0.005	—	—	—	0.056

† Accuracy estimates for first and second shell: $R \pm 0.02 \text{ \AA}$, $N \pm 20\%$.

‡ Accuracy estimates for third shell: $R \pm 0.06 \text{ \AA}$, $N \pm 60\%$.

§ Sample numbers correspond with those in Fig. 1.

|| Interatomic distance.

Coordination number.

†† Debye-Waller factor.

EXAFS spectra presented in Fig. 1. For convenient comparison, the RSFs relevant to each experimental parameter will be presented in a separate graph, along with the Fourier transforms of the theoretical spectra obtained from the fitting procedure.

Effect of pH Control

The effect of the pH control is demonstrated in Fig. 2, which compares the pH edge of a system where pH was allowed to drift during reaction to a pH edge where pH was held constant during reaction. All samples in Fig. 2 were reacted for 24 h at $I = 0.1 M$. Both pH edges show a relatively steep increase in Ni sorption above $\text{pH} \approx 6.5$. At pH values < 6.5 , essentially no difference in Ni sorption is observed between the two pH edges. In the steep part of the edge (pH values > 6.5), however, Ni sorption at a given pH is substantially higher for the edge with drifting pH than for the edge with constant pH. Two sets of data points from this

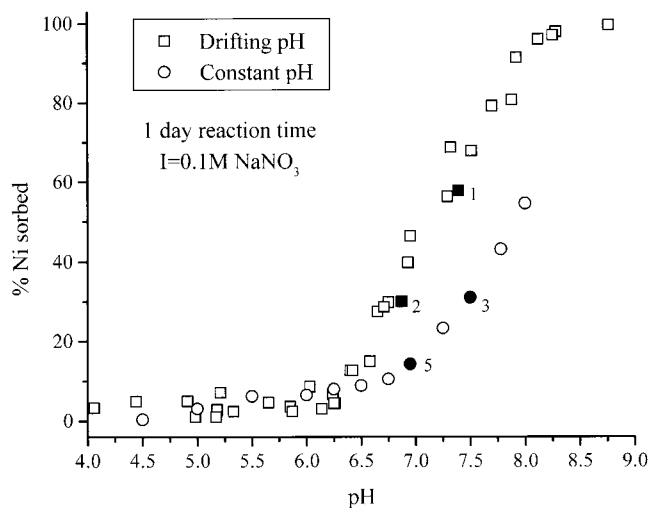


Fig. 2. Macroscopic data on the effect of pH control on Ni sorption to illite. The samples were reacted for 24 h at an ionic strength of $0.1 M$. Filled datapoints were analyzed by extended x-ray absorption fine structure spectroscopy (EXAFS); the sample numbers correspond with those in Fig. 1 and 3.

higher pH range were analyzed by EXAFS. Each set consisted of two data points that had similar final pH, but were reacted under different pH regimes. In all samples, the presence of Ni-Al LDH is observed, as indicated by the presence of a second neighbor peak in the radial structure functions (Fig. 3). The solid lines in Fig. 3 represent the Fourier transforms of the measured spectra, and the dotted lines those of the theoretical spectra derived with parameters obtained from the fitting procedure. A good agreement between the Fourier transformed EXAFS functions and the theoretical fits is observed for all samples. The intensities of the second (Ni-Ni/Al) shells suggest that formation of Ni-Al LDH is the main mode of Ni sorption in these samples, especially in the samples with drifting pH and in the sample with constant pH = 7.50, consistent with the results of Scheidegger et al. (1997, 1998).

The second shell in the RSF of the constant pH 6.95

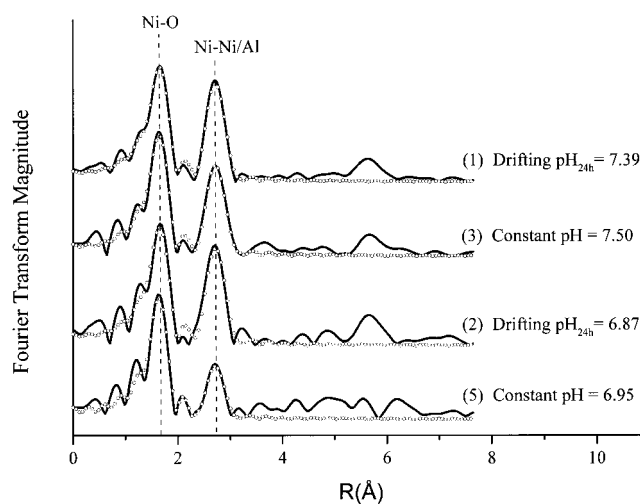


Fig. 3. Radial structure functions of the filled datapoints in Fig. 2. The solid lines represent the Fourier transforms of the measured spectra, and the dotted lines those of the theoretical spectra derived with parameters obtained from the fitting procedure. The radial structure functions are uncorrected for phase shift, and were obtained by Fourier transformation over $\Delta k = 3.2$ to 13.6 \AA^{-1} . Sample numbers (in parentheses) correspond with those in Fig. 1 and 2.

sample is smaller than that of the constant pH 7.50 sample (Fig. 3). Since the reaction time was the same for these samples and the amount of Ni sorbed was larger at pH 7.50 than at pH 6.95, this indicates that the rate of Ni-Al LDH formation increases with increasing pH. The enhanced formation rate of Ni-Al LDH with increasing pH may explain why Ni sorption above pH 6.5 is higher in the edge with drifting pH than in the edge with constant pH, as follows. In a preliminary Ni-illite sorption experiment using a pH-stat apparatus, it was found that base was needed to maintain a constant pH of 7.50 over time. This indicates that formation of Ni-Al LDH is accompanied by release of H⁺ ions into solution, although part of the base consumption in this experiment will have been due to illite dissolution, since the point of zero charge of illite is <7.50. Figure 4 shows Ni pH edges with non controlled pH for reaction times of 1 and 8 d. The arrows in this figure track the drift in pH and Ni sorption between 1 and 8 d of reaction for three samples in the pH range where Ni-Al LDH formation is observed. In all cases, we observe a pH drift to lower values that is accompanied by an increase in Ni sorption with time, consistent with the observation from the pH-stat experiment that Ni-Al LDH formation leads to H⁺ release into solution. These experimental results indicate that when pH is not controlled, high initial pHs continuously decrease with time due to Ni-Al LDH formation and illite dissolution. As a result, the pH measured after a 24 h reaction time, which is plotted on the x axis in Fig. 2, is lower than the initial pH at the start of the 24-h reaction time when pH is allowed to drift. In the presence of a buffer, however, the pH is maintained at the desired level during the 24-h reaction period. As a result, samples reacted for 24 h at constant pH effectively have been exposed to a lower pH value than samples that reach this pH after 24 h in the drifting pH regime. Since Ni-Al LDH formation proceeds faster at higher pH, more Ni-Al LDH is formed in the drifting pH samples than would be expected based on the pH measured after 24 h of reaction. Comparison of the

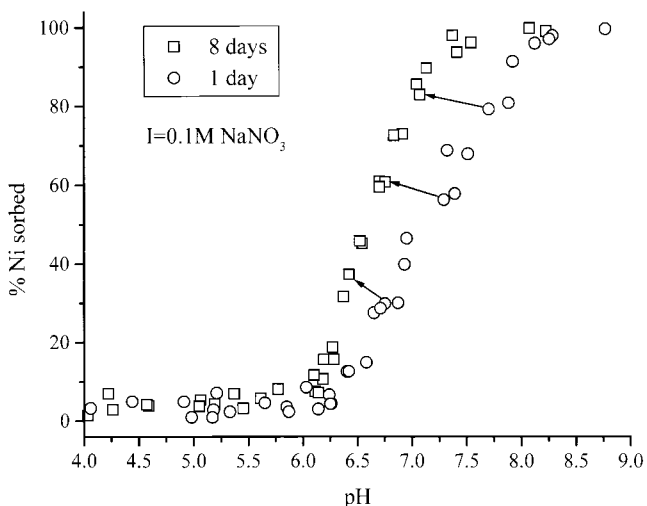


Fig. 4. pH edges after 24 h and 8 d of reaction in a system with drifting pH over time. The arrows track the pH drift and Ni sorption of select samples with time.

RSFs of drifting pH 6.87 vs. constant pH 7.50 shows that the intensity of the second peak is similar for these two samples. Since these samples have very similar Ni loadings (Fig. 1), this suggests that the effective pH of the drifting pH 6.87 sample during the 24-h reaction period was close to pH = 7.50.

A consequence of these findings is that modeling the kinetics of Ni sorption on clay minerals in the higher pH region will be more complicated when pH is not controlled. The change in pH with time will add an extra time dependency to the formation rate of Ni-Al LDH, since the formation rate is a function of pH. In turn, the change in pH over time itself will be affected by the formation rate of Ni-Al LDH, as well as by the rate of mineral dissolution, which also depends on pH, and is therefore also time dependent. Maintaining a constant pH over time will therefore significantly simplify the system in terms of modeling the Ni sorption kinetic behavior.

Effect of Reaction Time

The effect of reaction time is shown in Fig. 5 for the system with *I* = 0.1 M where pH was kept constant over time. At low pH values (pH < 6.25), no changes in the amount of Ni sorbed were observed between the samples taken at a reaction time of 3 h and those taken at longer reaction times. At pH values >6.25, however, Ni sorption continuously increased with time. The EXAFS data presented in Fig. 6 indicate that this is due to the formation of Ni-Al LDH. Two data points that had the same pH = 6.95 but were reacted with Ni for different times (1 d and 1 wk) show that the second Ni-Ni/Al peak in the radial structure function increases with time. This demonstrates the growth of the Ni-Al LDH precipitates with time, consistent with the time-resolved EXAFS study on Ni sorption on clay minerals presented by Scheidegger et al. (1998). We observe the formation of these phases at a pH value as low as 6.50 after a reaction time of 1 wk.

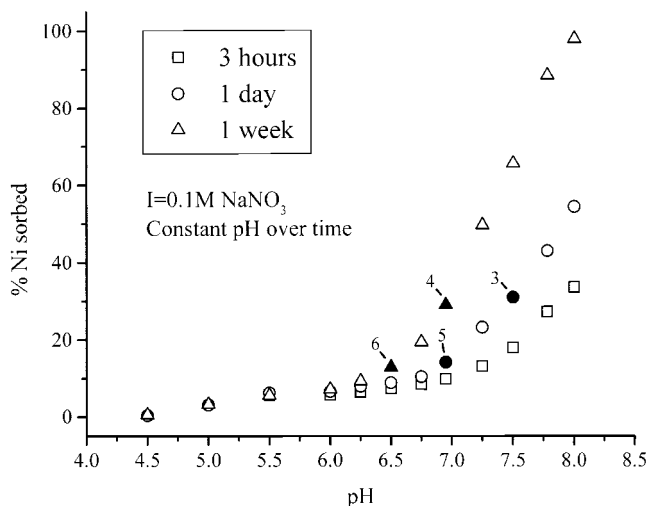


Fig. 5. Macroscopic data on the effect of reaction time on Ni sorption. The samples were reacted at constant pH and an ionic strength of 0.1 M. Filled datapoints were analyzed by extended x-ray absorption fine structure spectroscopy (EXAFS); the sample numbers correspond with those in Fig. 1 and 6.

Comparison of the RSFs of two data points (pH = 6.95 and 7.50) that have the same Ni loading but needed different reaction times (1 wk and 1 d, respectively) to reach this Ni loading level due to the difference in pH, shows that the intensity of the second (Ni-Ni/Al) shell is larger for pH = 7.50 than for pH = 6.95. The same holds true for the sample reacted at pH = 6.95 for 1 d vs. the sample reacted at pH = 6.50 for 1 wk, which also have similar Ni loadings. This demonstrates that the Ni bonding environment is different in these samples despite their very similar Ni loading levels. Three factors may explain this observation. First, formation of Ni-Al LDH phases as a Ni sorption mechanism may become more competitive with increasing pH relative to the other operative Ni sorption mechanisms (mononuclear inner- and outer-sphere adsorption at edge sites and planar sites). This may be related to the faster Ni-Al LDH precipitation at higher pH, which may make Ni-Al LDH formation more effective as a Ni sorption mechanism relative to Ni adsorption at the illite edge and planar sites. With increasing pH, Ni-Al LDH phases then would increasingly contribute to the total amount of sorbed Ni, which would lead to the observed increase in second neighbor scattering. An alternative explanation is related to diffusion to illite interlayer sites. The difference between the BET and EGME surface areas determined for our illite clay fraction (17 and 163 m² g⁻¹ for BET and EGME, respectively) indicates the presence of a fairly large internal surface area. The BET method accounts for the external surface area, whereas the EGME method measures both the internal and external surface area. The difference between the two methods therefore represents the internal surface area of the clay, which contains planar sites at which outer-sphere Ni sorption would occur. Diffusion of reactants to internal surface sites may be slow, occurring on time scales of weeks, as has been suggested for Cs sorption to illite (Comans et al., 1991). Therefore, due to the slower rate of Ni-Al LDH precipitation, and the longer

reaction time allowed for the lower pH samples (1 wk vs. 1 d for the higher pH samples with similar Ni loadings), a relatively large fraction of nickel metal ions in these samples may be adsorbed as mononuclear outer-sphere complexes at illite interlayer sites, which would explain the smaller second-neighbor scattering in these samples relative to the higher pH samples with similar Ni loadings. However, for samples with pH ≤ 6, where no Ni-Al LDH formation occurs (as will be shown later), no difference in Ni sorption is observed between 1-wk and 3-h reaction times (Fig. 2). This suggests that the illite interlayer sites are readily accessible, and that slow diffusion of Ni to illite interlayer sites does not play a role in the reduced second neighbor scattering observed for the samples reacted for 1 wk.

Secondly, the composition of the Ni-Al LDH phases may be different at the two different pH values. Since the EXAFS contributions resulting from second-neighbor Al scattering are partly out of phase with those resulting from second-neighbor Ni scattering (d'Espinoze de la Caillerie et al., 1995; Scheidegger et al., 1997), an increase in the Al content of the Ni-Al LDH phase would lead to an apparent decrease in overall second-neighbor scattering, and would therefore decrease the intensity of the second shell in the RSF (Scheinost and Sparks, 2000). As noted previously, the rate of formation of Ni-Al-LDH increases with increasing pH. The fast formation of Ni-Al LDH phases at pH 7.50 relative to pH 6.95 may lead to a lower Al content in the Ni-Al LDH phase formed at pH 7.50, since the amount of Al dissolved from the clay structure may be larger during 1 wk of reaction at pH 6.95 than during 1 d of reaction at pH 7.50. Unfortunately, it is not possible to make a reliable estimate of the $N_{\text{Ni-Ni}}/N_{\text{Ni-Al}}$ ratio from Ni-Al LDH EXAFS data, since the amplitude cancellation between the Ni and Al shells not only leads to apparent reduced second neighbor scattering, but also results in poorly constrained accuracies for the $N_{\text{Ni-Al}}$ and $R_{\text{Ni-Al}}$ values obtained from EXAFS data fitting (Scheidegger et al., 1998).

Thirdly, the average cluster size of the Ni-Al LDH precipitate may be larger at higher pH (i.e., shorter reaction time). This would lead to an increase in the average number of second neighbors, and would therefore increase second neighbor scattering. Since EXAFS probes the bonding environment of the central atom within an approximate 8 Å radius (B. Boyanov, 1998, personal communication), it is sensitive to Ni-Al LDH crystal size (with respect to $N_{\text{Ni-Ni}}$) only if the average radius of the Ni-Al LDH sheets is smaller than ~35 nm (A. Scheinost, 2000, personal communication). It should be noted, therefore, that a larger average Ni-Al LDH crystal size is indicated by larger second neighbor scattering only if the precipitates are within this size scale. In an EXAFS study on Co sorption on kaolinite, where Co(OH)₂-like phases formed that are similar to the Ni-Al LDH phases we observe, O'Day et al. (1994) hypothesized that the formation of smaller precipitate clusters occurred over time on the kaolinite clay fraction (<2-μm fraction). Similar to our findings, a decrease in Co-Co scattering for long-term samples (reacted for

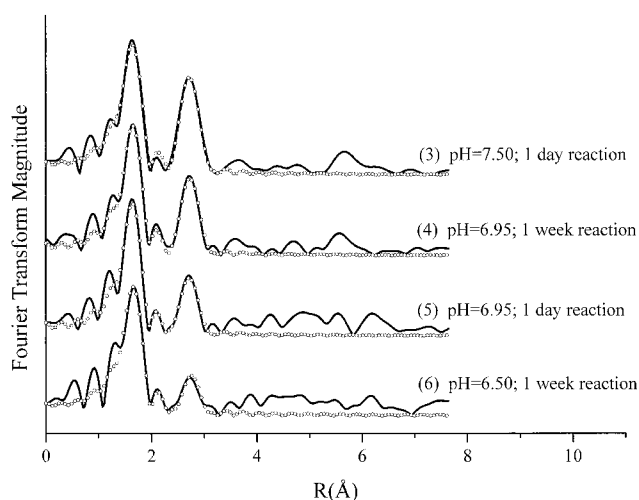


Fig. 6. Radial structure functions RSFs (uncorrected for phase shift) of the filled datapoints in Fig. 5. Fourier transformation was performed over $\Delta k = 3.2$ to 13.6 \AA^{-1} for all samples. The solid lines are the Fourier transforms of the measured spectra, and the dotted lines those of the theoretical spectra. The sample numbers in brackets correspond with those in Fig. 1 and 5.

45 d) was observed as compared with short-term samples (reacted for 24 h). O'Day et al. (1994) hypothesized that the short-term sorption products may be large, metastable multinuclear complexes, or a disordered hydrous precipitate resulting from fast Co sorption from solution. The surface species may reorganize in time to form smaller complexes that are bonded directly to the surface, which would account for the decrease in average Co backscattering with time. This mechanism may also occur in our system and explain the lower Ni-Ni scattering for the 7-d sample (pH = 6.95) as compared with the 24-h sample (pH = 7.50). An important difference in our study compared with the study by O'Day et al. (1994), however, is that we compare the effect of time for samples with different pHs, whereas pH was the same for the 24-h and 48-d samples in O'Day's study, which both had essentially 100% Co sorbed. Our data show that Ni-Al LDH precipitation proceeds faster at higher pH. A fast precipitation process generally leads to many small crystals, whereas slow precipitation causes a few large crystals to grow (Morse and Casey, 1988; Putnis, 1992). This would lead to a higher average $N_{\text{Ni-Ni}}$ for low pH (slow precipitation) as compared with high pH (fast precipitation) in our samples. Since we observed the opposite, it is not likely that differences in crystal size can explain the observed difference in Ni-Ni scattering between these samples. More likely, the possible differences with respect to the amount or composition of the Ni-Al LDH phases discussed above are responsible for the observed difference.

Effect of Ionic Strength

Ionic strength has a substantial effect on Ni sorption as a function of pH, as demonstrated in Fig. 7. At any given pH value, Ni sorption is higher for $I = 0.003 M$ than for $I = 0.1 M$. The radial structure functions of selected samples in Fig. 7 are given in Fig. 8. The samples selected had the same pH but different ionic strengths.

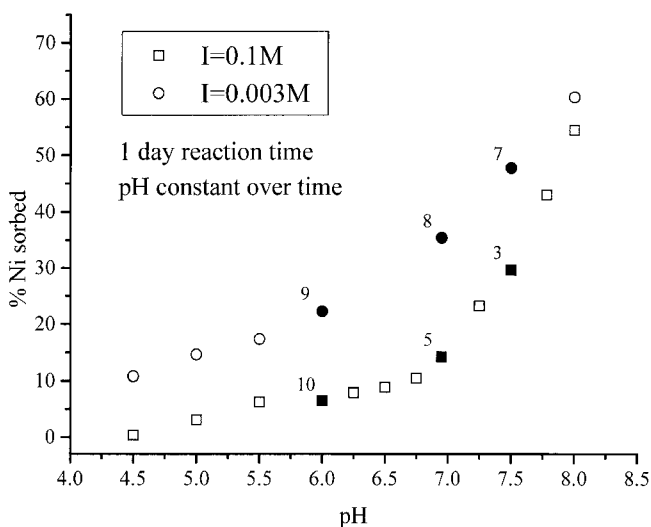


Fig. 7. Macroscopic data on the effect of ionic strength on Ni sorption. The samples were reacted for 24 h at constant pH. Filled datapoints were analyzed by extended x-ray absorption fine structure spectroscopy (EXAFS); the sample numbers correspond with those in Fig. 1 and 8.

At pH 6.0, no differences between the RSFs of low I and high I samples are apparent above the noise level. The noise level of the $I = 0.1 M$ sample at this pH is relatively high, however, due to its low Ni loading level. Possible differences with the $I = 0.003 M$ sample may therefore not be visible.

The EXAFS results of pH = 6.95 and 7.50 show the formation of Ni-Al LDH precipitates at both low I and high I . However, at both pH values, the second Ni-Ni/Al peak is smaller for $I = 0.003 M$ than for $I = 0.1 M$, although the total Ni uptake is higher at $I = 0.003 M$. This suggests substantial outer-sphere adsorption of Ni at low ionic strength. The potential of illite for cation exchange is mainly associated with the interlayer region, which contains planar sites at which outer-sphere Ni sorption would occur. As noted above, the illite clay fraction used in this study contains a fairly large interlayer region, as indicated by the difference between the BET and EGME surface areas (17 and $163 \text{ m}^2 \text{ g}^{-1}$ for BET and EGME, respectively). At high ionic strength ($I = 0.1 M$), outer-sphere Ni sorption is suppressed due to the high concentration of Na ions, that compete with Ni ions for planar sites. At low ionic strength ($I = 0.003 M$) the concentration of Na ions is low, and Ni can more effectively compete for the outer-sphere sorption sites. The EXAFS data suggest that the resultant increase in outer-sphere Ni complexes leads to a decrease in the importance of Ni-Al LDH formation as a Ni sorption mechanism, as reflected in the smaller second peak in the RSFs. A similar observation was made by Papelis and Hayes (1996) for Co sorption on montmorillonite, which is a strongly swelling clay mineral with an even higher potential for outer-sphere metal sorption than illite. Note that it is still possible in our system that the absolute amount of Ni-Al LDH formed is the same at low and high I . The total Ni sorption is higher at low I and EXAFS provides an average bonding environment of all sorbed Ni atoms. An increase in outer-sphere Ni sorption with the same amount of Ni present in Ni-Al

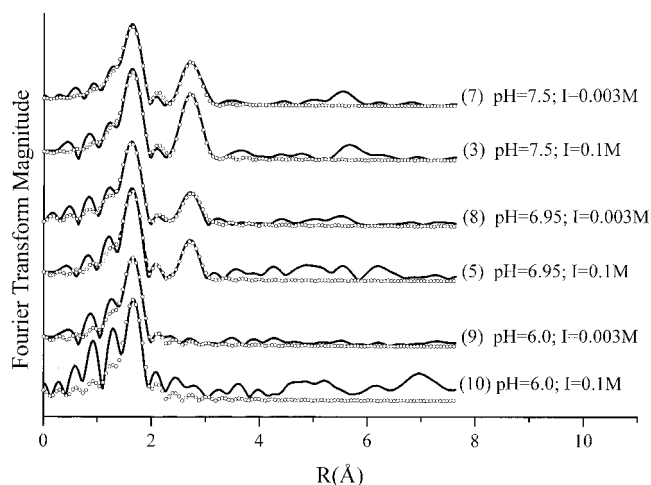


Fig. 8. Radial structure functions (uncorrected for phase shift) of the filled datapoints in Fig. 7. Fourier transformation was performed over $\Delta k = 3.2$ to 13.6 \AA^{-1} . The solid lines are the Fourier transforms of the measured spectra, and the dotted lines those of the theoretical spectra. The sample numbers in brackets correspond with those in Fig. 1 and 7.

LDH will therefore lead to a decrease in the relative contribution of Ni-Al LDH to the total amount of Ni sorbed, which would result in the observed lower (average) Ni-Ni scattering.

CONCLUSIONS

Our EXAFS data show that the formation of mixed Ni-Al LDH precipitates is an important Ni sorption mechanism in Ni-illite systems at pH values >6.25. The rate of formation of these phases was found to increase with increasing pH, and the precipitates continued to grow with time. Comparison between samples that had the same Ni loading, but were reacted for different reaction times and at different pH values, showed enhanced second neighbor scattering at higher pH. This either indicated a relative increase in the importance of Ni-Al LDH precipitation as a Ni sorption mechanism relative to other (mononuclear) Ni sorption mechanisms with increasing pH (shorter reaction time), and/or a higher Al content in the Ni-Al LDH phase formed at longer reaction times (lower pH). Our data suggest that at low Na concentrations (i.e., low ionic strength), significant outer-sphere Ni sorption occurred, leading to an overall increase in Ni sorption and a reduced contribution of Ni-Al LDH phases to the overall amount of Ni sorbed.

ACKNOWLEDGMENTS

The authors appreciate the support of this research by the USDA-NRICGP, the State of Delaware, and the DuPont Company. E.J. Elzinga is grateful for a University of Delaware College of Agricultural and Natural Resources Competitive Graduate Fellowship. Thanks are also extended to Drs. R.G. Ford and A.C. Scheinost, and to D.R. Roberts for their critical comments on a first draft of this manuscript.

REFERENCES

- Baeyens, B., and M.H. Bradbury. 1995. A quantitative mechanistic description of Ni, Zn and Ca sorption on Na-montmorillonite. Report PSI Ber. 95-11. Paul Scherrer Institut, Villigen, Switzerland.
- Bargar, J.R., G.E. Brown, Jr., and G.A. Parks. 1998. Surface complexation of Pb(II) at oxide-water interfaces: III. XAFS determination of Pb(II) and Pb(II)-chloro adsorption complexes on goethite and alumina. *Geochim. Cosmochim. Acta* 62:193-207.
- Benjamin, M.M., and J.O. Leckie. 1982. Effects of complexation by Cl, SO₄, and S₂O₃ on adsorption behavior of Cd on oxide surfaces. *Environ. Sci. Technol.* 16:162-170.
- Bolt, G.H., M.G.M. Bruggenwert, and A. Kamphorst. 1979. Adsorption of cations by soil. p. 54-90. *In* G.H. Bolt and M.G.M. Bruggenwert (ed.) *Soil chemistry. A. Basic elements*. Elsevier, Amsterdam, the Netherlands.
- Bouldin, C., L. Furenlid, and T. Elam. 1995. MacXAFS—An EXAFS analysis package for the MacIntosh. *Physica B* 209:190-192.
- Comans, R.N.J., M. Haller, and P. Depreter. 1991. Sorption of cesium on illite—Nonequilibrium behavior and reversibility. *Geochim. Cosmochim. Acta* 55:433-440.
- d'Espinose de la Caillerie, J.B., M. Kermarec, and O. Clause. 1995. Impregnation of g-alumina with Ni(II) and Co(II) ions at neutral pH: Hydrotalcite-type formation and characterization. *J. Am. Chem. Soc.* 117:11471-11481.
- Fanning, D.S., V.Z. Keramidias, and M.A. El-Dosoky. 1989. Micas. p. 551-634. *In* J.B. Dixon and S.B. Weed (ed.) *Minerals in soil environments*. SSSA Book Ser. 1. SSSA, Madison, WI.
- Ford, R.G., A.C. Scheinost, K.G. Scheckel, and D.L. Sparks. 1999. The link between clay mineral weathering and the stabilization of Ni surface precipitates. *Environ. Sci. Technol.* 33:3140-3144.
- Génin, P., A. Delahaye-Vidal, F. Portemer, K. Tekaiia-Elhissen, and M. Figlarz. 1991. *Eur. J. Solid State Inorg. Chem.* 28:505-518.
- Jackson, M.L. 1956. *Soil chemical analysis: Advanced course*. M.L. Jackson, Madison, WI.
- McBride, M.B. 1994. *Environmental chemistry of soils*. Oxford Univ. Press, New York.
- Morse, J.W., and W.H. Casey. 1988. Ostwald processes and mineral paragenesis in sediments. *Am. J. Sci.* 288:537-560.
- O'Day, P.A., G.E. Brown, Jr., and G.A. Parks. 1994. X-ray absorption spectroscopy of cobalt(II) multinuclear surface complexes and surface precipitates on kaolinite. *J. Colloid Interface Sci.* 165:269-289.
- O'Day, P.A., C.J. Chisholm-Brause, S.N. Towle, G.A. Parks, and G.E. Brown, Jr. 1996. X-ray absorption spectroscopy of Co(II) sorption complexes on quartz (α -SiO₂) and rutile (TiO₂). *Geochim. Cosmochim. Acta* 60:2515-2532.
- Papelis, C., and K.F. Hayes. 1996. Distinguishing between interlayer and external sorption sites of clay minerals using X-ray absorption spectroscopy. *Colloids Surf. A* 107:89-96.
- Putnis, A. 1992. *Introduction to mineral sciences*. Cambridge Univ. Press, Cambridge, UK.
- Roberts, D.R., A.M. Scheidegger, and D.L. Sparks. 1999. Kinetics of mixed Ni-Al precipitate formation on a soil clay fraction. *Environ. Sci. Technol.* 33:3749-3754.
- Roe, A.L., K.F. Hayes, C.J. Chisholm-Brause, G.E. Brown, Jr., G.A. Parks, K.O. Hodgson, and J.O. Leckie. 1991. In situ X-ray absorption study of lead ion surface complexes at the goethite-water interface. *Langmuir* 7:367-373.
- Scheidegger, A.M., G.M. Lamble, and D.L. Sparks. 1997. Spectroscopic evidence for the formation of mixed-cation hydroxide phases upon metal sorption on clays and aluminum oxides. *J. Colloid Interface Sci.* 186:118-128.
- Scheidegger, A.M., D.G. Strawn, G.M. Lamble, and D.L. Sparks. 1998. The kinetics of mixed Ni-Al Hydroxide formation on clays and aluminum oxides: A time-resolved XAFS study. *Geochim. Cosmochim. Acta* 62:2233-2245.
- Scheinost, A.C., R.G. Ford, and D.L. Sparks. 1999. The role of Al in the formation of secondary Ni precipitates on pyrophyllite, gibbsite, talc and amorphous silica: A DRS study. *Geochim. Cosmochim. Acta* 63:3193-3203.
- Scheinost, A.C., and D.L. Sparks. 2000. Formation of layered single- and double-metal hydroxide precipitates at the mineral/water interface: A multiple-scattering XAFS analysis. *J. Colloid Interface Sci.* 223:167-178.
- Sparks, D.L. 1995. *Environmental soil chemistry*. Academic Press, San Diego, CA.
- Sposito, G. 1989. *The chemistry of soils*. Oxford Univ. Press, New York.
- Srodin, J., and D.D. Eberl. 1984. Illite. p. 495-544. *In* S.W. Bailey (ed.) *Micas*. Mineralogical Soc. Am., Washington, DC.
- Strawn, D.G., A.M. Scheidegger, and D.L. Sparks. 1998. Kinetics and mechanisms of Pb(II) sorption and desorption at the aluminum oxide-water interface. *Environ. Sci. Technol.* 32:2596-2601.
- Strawn, D.G., and D.L. Sparks. 1999. The use of XAFS to distinguish between inner- and outer-sphere lead adsorption complexes on montmorillonite. *J. Colloid Interface Sci.* 216:257-269.
- Thompson, H.A., G.A. Parks, and G.E. Brown, Jr. 1999. Dynamic interactions of dissolution, surface adsorption, and precipitation in an aging cobalt(II)-clay-water system. *Geochim. Cosmochim. Acta* 63:1767-1779.
- Towle, S.N., J.R. Bargar, G.E. Brown, Jr., and G.A. Parks. 1997. Surface precipitation of Co(II) (aq) on Al₂O₃. *J. Colloid Interface Sci.* 187:62-82.
- Zabinsky, S.I., J.J. Rehr, A. Ankudinov, R.C. Albers, and M.J. Eller. 1995. Multiple-scattering calculations of X-ray absorption spectra. *Phys. Rev. B* 52:2995-3006.
- Zachara, J.M., S.C. Smith, J.P. McKinley, and C.T. Resch. 1993. Cadmium sorption on specimen and soil smectites in sodium and calcium electrolytes. *Soil Sci. Soc. Am. J.* 57:1491-1501.